Freeform lens design for LED collimating illumination

Jin-Jia Chen,[1,*] Te-Yuan Wang,[1] Kuang-Lung Huang,[2] Te-Shu Liu,[1] Ming-Da Tsai,[1] and Chin-Tang Lin[1]

[1] *Department of Electrical Engineering, National Changhua University of Education, 2 ShiDa Road, Changhua 50074, Taiwan*

[2] *Department of Electro-Optical and Energy Engineering, Mingdao University, 369 Wen Hwa Road, Peetow, Changhua 52345, Taiwan*

[*] *jjchen@cc.ncue.edu.tw*

Abstract: We present a simple freeform lens design method for an application to LED collimating illumination. The method is derived from a basic geometric-optics analysis and construction approach. By using this method, a highly collimating lens with LED chip size of 1.0 mm×1.0 mm and optical simulation efficiency of 86.5% under a view angle of ± 5 deg is constructed. To verify the practical performance of the lens, a prototype of the collimator lens is also made, and an optical efficiency of 90.3% with a beam angle of 4.75 deg is measured.

OCIS codes: (220.2740) Geometric optical design; (220.4298) Nonimaging optics; (220.2945) Illumination design; (230.3670) Light-emitting diodes.

References and links

1. H. Ries and J. Muschaweck, "Tailored freeform optical surfaces," J. Opt. Soc. Am. A **19**(3), 590–595 (2002).
2. P. Benítez, J. C. Miñano, J. Blen, R. Mohedano, J. Chaves, O. Dross, M. Hernández, and W. Falicoff, "Simultaneous multiple surface optical design method in three dimensions," Opt. Eng. **43**(7), 1489–1502 (2004).
3. Y. Ding, X. Liu, Z. R. Zheng, and P. F. Gu, "Freeform LED lens for uniform illumination," Opt. Express **16**(17), 12958–12966 (2008).
4. L. Sun, S. Jin, and S. Cen, "Free-form microlens for illumination applications," Appl. Opt. **48**(29), 5520–5527 (2009).
5. F. R. Fournier, W. J. Cassarly, and J. P. Rolland, "Fast freeform reflector generation usingsource-target maps," Opt. Express **18**(5), 5295–5304 (2010).
6. W. Zhang, Q. Liu, H. Gao, and F. Yu, "Free-form reflector optimization for general lighting," Opt. Eng. **49**(6), 063003 (2010).
7. G. Wang, L. Wang, L. Li, D. Wang, and Y. Zhang, "Secondary optical lens designed in the method of source-target mapping," Appl. Opt. **50**(21), 4031–4036 (2011).
8. V. Medvedev and W. A. Parkyn, Jr., "Screen illumination apparatus and method," US Patent 6166860 (2000).
9. D. Weigert and D. Chin, "Spotlight with an adjustable angle of radiation and with an aspherical front lens," US Patent 6499862 B1 (2002).
10. A. Domhardt, S. Weingaertner, U. Rohlfing, and U. Lemmer, "TIR Optics for non-rotationally symmetric illumination Design," Proc. SPIE **7103**, 710304, 710304-11 (2008).
11. J.-J. Chen and C.-T. Lin, "Freeform surface design for a light-emitting diode–based collimating lens," Opt. Eng. **49**(9), 093001 (2010).
12. D. Vázquez-Moliní, M. González-Montes, A. Álvarez, and E. Bernabéu, "High-efficiency light-emitting diode collimator," Opt. Eng. **49**(12), 123001 (2010).
13. J. Chaves, *Introduction to Nonimaging Optics* (CRC Press, Boca Raton, 2008), Chap. 8.
14. L. Piegl and W. Tiller, *The NURBS Book* (Springer-Verlag, Berlin, 1997).

1. Introduction

In recent years, due to the speedy growth of LED light sources in general illumination applications, such as LED bulbs, spotlights, street lights, vehicle headlamps, and etc., many lamp fabricators and designers have proposed various LED luminaire techniques. LED luminaires are generally and purposely designed to redirect light rays to produce a specific distribution, and many methods aim this goal with employing standard conic or aspherical optical surfaces. However, when high optical performance or compact volume is desired, LED luminaires should be designed with irregular or freeform surfaces. Thus, many freeform

#164581 - $15.00 USD Received 13 Mar 2012; revised 7 Apr 2012; accepted 7 Apr 2012; published 26 Apr 2012

surface design methods [1–7] have been proposed in the past decade. Nevertheless, most methods [1, 3–5, 7] convert the design problems into suitable group differential equations through a mapping between the light source and the target, and therefore need to solve solution numerically. Other methods [2, 6], though not using the mapping approach, have complex mathematic derivation and operation, and even need further optimization.

As concerns the collimator lens, which has many versatile applications to spotlight, flashlight, vehicle headlamps, and LCD projector light, conventional methods [8–9] adopt multiple conic or aspherical optical elements to realize the lens. However, its volume is large, and light rays cannot be effectively utilized. Also, the composed elements need rigorous alignment to obtain good performance. Since the freeform total internal reflection (TIR) structure can concrete all elements into a single body and achieve high performance with compact volume, therefore, it has attracted many interesting applications [10–12] recently.

In this paper, we propose a method, which is derived from a basic and simple geometric-optics analysis and construction approach, to construct freeform surfaces without using complex derivations. Though this method has been used to design a TIR collimator lens [11], the detailed and complete outline of the method is given in this paper, and an application to a novel compact LED collimator lens with ellipsoidal and freeform profile is also given. In addition to the simulation results, a prototype is also made to practically verify the performance of the lens. As compared with the TIR lens in [11], the collimator lens in this paper has better optical efficiency and smaller spot size under same lens dimensions. In addition, the lens in this paper is more easily fabricated than that in [11] due to an acute angle existing in the latter.

2. Proposed methodology

The proposed freeform surface design method consists of two processes, the geometric-optics analysis and the freeform-surface construction. The purpose of the geometric-optics analysis is to find the tangential vector, which is used to calculate the associated reflective or refractive point on a freeform optical surface. Once the tangential vector at each reflective or refractive point is calculated, a two-dimensional (2D) contour of the surface can be constructed following the procedure given in Section 2.2. Finally, a three-dimensional (3D) freeform surface is obtained by rotating the 2D contour around the axis. Detailed analysis and construction processes are depicted in the follows.

2.1 Geometric-optics analysis

Optical surfaces are normally classified into reflective and refractive surfaces, and therefore the associated geometric-optics analysis for the reflective and refractive surfaces will be given, respectively.

2.1.1 Analysis for the reflective surface

A reflective surface can shift the direction of an incident light ray to a specific direction or a point based on the reflection law. The basic geometric-optics relation for a reflective surface shifting a light ray emitted from a light source to a specific direction θ_P' is depicted in Fig. 1(a), where P is an arbitrary point on the surface and the angle θ_P stands for the direction of the incident light ray to the x axis. Assume the incident and reflective angles to be θ_i and θ_r, respectively; then, from Fig. 1(a), the intersection angle θ_T of a tangential vector $\overline{T}$ at point P can be expressed as

$$\theta_T = \frac{\pi}{2} + \left(\theta_i - \theta_P\right) \tag{1}$$

In addition, from Fig. 1(a), we obtain the following relation:

$$\theta_i + \theta_r = \theta_P + \theta_P' \tag{2}$$

#164581 - $15.00 USD Received 13 Mar 2012; revised 7 Apr 2012; accepted 7 Apr 2012; published 26 Apr 2012

According to the reflection law, the incident angle θ_i must be equal to the reflective angle θ_r, and therefore we have

$$\theta_i = \theta_r = \frac{(\theta_P + \theta'_P)}{2} \tag{3}$$

Substituting Eq. (3) into Eq. (1), we obtain

$$\theta_T = \frac{\pi}{2} + \frac{(\theta'_P - \theta_P)}{2}. \tag{4}$$

From Eq. (4), if θ_P and θ'_P are known, the intersection angle θ_T can be solved, and the tangential slope and vector at point P can be given by

$$\text{Slope} = \tan\left[\frac{\pi}{2} + \frac{(\theta'_P - \theta_P)}{2}\right] = -\cot\left(\frac{\theta'_P - \theta_P}{2}\right) \tag{5}$$

and

$$\overline{T} = [1, \tan\theta_T] = \left[1, -\cot\left(\frac{\theta'_P - \theta_P}{2}\right)\right]. \tag{6}$$

In the other case, when the incident light ray is redirected to a specific point F by the reflective surface, as shown in Fig. 1(b), the tangential slope at point P is also given by Eq. (5), whereas the angle θ'_P is given by

$$\theta'_P = \tan^{-1}\left[\frac{\overline{FQ}}{\overline{PQ}}\right] \tag{7}$$

Since point F is initially given and point P is found from the 2D-contour construction in Section 2.2; therefore, $\overline{FQ}$, $\overline{PQ}$, and hence the tangential slope at point P can be calculated.

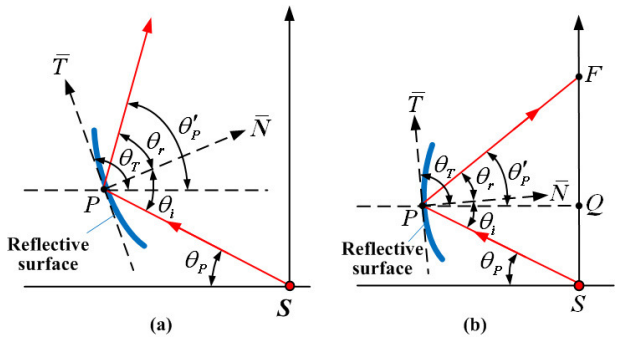

Fig. 1. Geometric-optics relation for an arbitrary reflective surface. (a) For a surface reflecting light rays to a specific direction. (b) For a surface focusing light rays to a specific point.

2.1.2 Analysis for the refractive surface

Similarly, a refractive sureface can shift the direction of an incident light ray to a specific direction or a point based on the Snell's law. The basic geometric-optics relation for a refractive surface shifting a light ray emitted from a source to a specific direction θ'_P is depicted in Fig. 2(a). Assume the incident and refractive angles to be θ_i and θ_t, respectively; then from Fig. 2(a), the refractive angle can be expressed as

#164581 - $15.00 USD Received 13 Mar 2012; revised 7 Apr 2012; accepted 7 Apr 2012; published 26 Apr 2012

$$\theta_t = \frac{\pi}{2} - \left(\theta'_P - \theta_T\right) \tag{8}$$

In addition, from this figure we obtain the following relation:

$$\theta_i = \left(\theta_P + \theta_T\right) - \frac{\pi}{2} \tag{9}$$

Since point *P* is a refractive point, thus θ_i and θ_t must satisfy Snell's law, that is,

$$n_1 \sin\theta_i = n_2 \sin\theta_t \tag{10}$$

In Eq. (10), n_1 and n_2 are the refractive indices of the two media in Fig. 2. Substituting Eqs. (8) and (9) into Eq. (10) and rearranging the resultant equation, we obtain the intersection angle of the tangential vector $\bar{T}$ at point *P* as

$$\theta_T = \tan^{-1}\left(\frac{n_1 \cos\theta_P + n_2 \cos\theta'_P}{n_1 \sin\theta_P - n_2 \sin\theta'_P}\right), \tag{11}$$

The tangential slope and vector at point *P* can also be expressed as

$$\text{Slope} = \tan\theta_T = \frac{n_1 \cos\theta_P + n_2 \cos\theta'_P}{n_1 \sin\theta_P - n_2 \sin\theta'_P} \tag{12}$$

and

$$\bar{T} = \left[1, \tan\theta_T\right] = \left[1, \frac{n_1 \cos\theta_P + n_2 \cos\theta'_P}{n_1 \sin\theta_P - n_2 \sin\theta'_P}\right]. \tag{13}$$

In the other case, when a light ray emitted from the light source is redirected to a specific point *F* by the refractive surface, as shown in Fig. 2(b), the tangential slope at point *P* is also given by Eq. (12), whereas the angle θ'_P is given by $\theta'_P = \tan^{-1}\left[\overline{FQ}/\overline{PQ}\right]$.

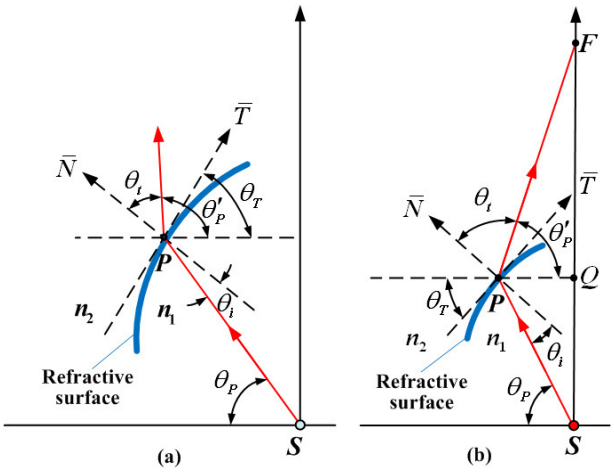

Fig. 2. Geometric-optics relation for an arbitrary refractive surface. (a) For a surface refracting light rays to a specific direction. (b) For a surface focusing light rays to a specific point.

2.2 Freeform surface construction

According to previous geometric-optics analysis, we can use the following procedure, which is shown in Fig. 3, to find each reflective or refractive point on a freeform surface so that its 2D contour can be constructed step by step. Figure 3 illustrates light rays emitted from a light

#164581 - $15.00 USD Received 13 Mar 2012; revised 7 Apr 2012; accepted 7 Apr 2012; published 26 Apr 2012

source and redirected by a freeform reflective surface to a prescribed direction parallel to the optical axis. As shown in Fig. 3, red lines marked with i_0, i_1, i_2 and i_3 stand for arbitrarily given light rays, which are emitted from the light source S and then hit the reflective surface at points of P_0, P_1, P_2, and P_3, respectively. Point P_0 is the initial point of the 2D contour, and is given by the designer according to the wanted surface dimension. The blue dashed lines $\overline{T}_0$, $\overline{T}_1$, and $\overline{T}_2$, which are used to construct the 2D contour, stand for the tangential vector at point P_0, P_1, and P_2, respectively.

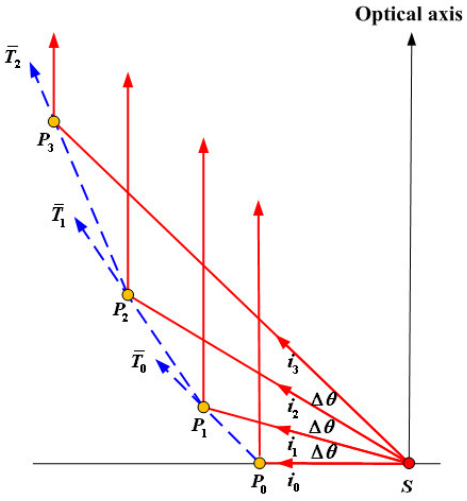

Fig. 3. Two-dimensional contour construction for a freeform reflective surface.

The procedure to construct the 2D contour is stated as the follows. First, give the initial point P_0 and use Eq. (5) to find the tangential vector $\overline{T}_0$ at point P_0, where θ'_P is assigned to be $\pi/2$ for the incident light ray i_0 reflected by the surface to a direction parallel to the optical axis. Next, find point P_1, which is located at the intersection point of the incident light ray i_1 and the tangential vector $\overline{T}_0$. The next, use Eq. (5) again to find the tangential vector $\overline{T}_1$ at the point P_1. Then find point P_2, which is located at the intersection point of the incident light ray i_2 and the tangential vector $\overline{T}_1$. Repeat the above process till all the *P*-points are found, and the whole 2D contour of the freeform surface can be constructed with the help of CAD software program and the obtained *P*-points. However, to retain the slope at each point, the contour between any two consecutive *P*-points should be constructed using a interpolation approach based on a high-degree polynomial [13] or B-spline functions [14].

For illustration, a third-degree polynomial is given by

$$p(x) = ax^3 + bx^2 + cx + d \tag{14}$$

If the coordinates of points P_n and P_{n+1} are given by (P_{n1}, P_{n2}) and $\left(P_{(n+1)1}, P_{(n+1)2}\right)$, then we have the following relations:

$$\begin{aligned} P_{n2} &= aP_{n1}^3 + bP_{n1}^2 + cP_{n1} + d \\ P_{(n+1)2} &= aP_{(n+1)1}^3 + bP_{(n+1)1}^2 + cP_{(n+1)1} + d \end{aligned} \tag{15}$$

and

#164581 - $15.00 USD Received 13 Mar 2012; revised 7 Apr 2012; accepted 7 Apr 2012; published 26 Apr 2012

$$\frac{dp\left(P_{n1}\right)}{dx} = \tan\theta_{T_n} = 3aP_{n1}^2 + 2bP_{n1} + c$$
$$\frac{dp\left(P_{(n+1)1}\right)}{dx} = \tan\theta_{T_{n+1}} = 3aP_{(n+1)1}^2 + 2bP_{(n+1)1} + c \tag{16}$$

By simultaneously solving Eqs. (15) and (16) to give the value of a, b, c, and d, the contour between points P_n and P_{n+1} is thus given by $\left(x, p\left(x\right)\right)$ with $P_{(n+1)1} < x < P_{n1}$. Once the 2D contour is obtained, the 3D axis-symmetrical freeform surface can therefore be established by rotating the 2D contour about the optical axis.

3. Application to construct a compact collimator lens

For illustrating the application of the method, we employ it to construct a compact LED collimator lens. Both the construction process and computer simulation of the lens are stated in detail in the following subsections.

3.1 Construction of the lens

The 2D plot of the proposed compact collimator lens is sketched in Fig. 4, where only half of the lens is sketched because of the axis-symmetrical structure. As shown in Fig. 4, this lens consists of five reflective/refractive surfaces, which are respectively marked with a circled number. Surface ① is a spherical refractive surface, surface ② is an ellipsoidal reflective surface, and the other three surfaces are refractive surfaces with freeform profiles. In addition, the light source S is located at the first focal point of the ellipsoidal surface ②, and point F is its secondary focal point. For conveniently explaining the function for each surface, we categorize light rays emitted from the source S into three groups, and the optical property of each group light rays is stated in the following:

1) Light rays of group 1 with a spread angle of θ_a will enter the zone 1 of the collimator lens through the spherical surface ① firstly, and then are reflected to point F by the ellipsoidal surface ②. While before arriving point F, they will hit the freeform surface ⑤ firstly and be diverted to parallel the optical axis.

2) Light rays of group 2 with a spread angle of θ_b will enter the zone 2 of the collimator lens through the surface ① firstly. Then they are refracted to parallel the optical axis by the freeform surface ③.

3) Light rays of group 3 with a spread angle of θ_c will enter the zone 3 of the collimator lens through the freeform surface ④ and then are focused to point F. While before arriving point F, they will hit the freeform surface ⑤ firstly and be diverted to parallel the optical axis.

Therefore, all the light rays emitted from the light source S are finally collimated to the optical axis through the lens. In addition, all the surfaces, including surfaces ① and ②, can be constructed by using the method depicted in Section 2.2.

#164581 - $15.00 USD Received 13 Mar 2012; revised 7 Apr 2012; accepted 7 Apr 2012; published 26 Apr 2012

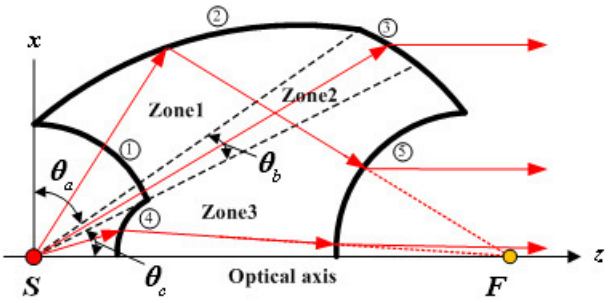

Fig. 4. The two-dimensional plot of the compact collimator lens.

The detailed construction process of the five surfaces is given in the following:

1) First, decide the dimension of the entrance aperture on the left of the lens. In other words, to give the initial point of the surface ②.

2) Then, use the initial point to construct the surface ② that can focus light rays in zone 1 to point *F*.

3) Next, construct the spherical surface ① and let its center be located at the light source *S*. Thus, light rays entering this surface will not be deflected.

4) Next, construct the surface ④ with its construction initial-point (or vertex) located at the optical axis to focus light rays in zone 3 to the point *F*.

5) Next, construct the surface ⑤ with its construction initial-point located at the optical axis to make light rays in zone 1 and zone 3 parallel to the optical axis when passing through the surface. The point is the dimension of surface ⑤ should be made larger as possibly to promote the optical efficiency but should not cross over the boundary between zone 2 and zone 3; otherwise, some light rays in zone 2 will hit the surface ⑤ and encounter total internal reflection.

6) Finally, construct the surface ③ with the end point of the surface ⑤ as its construction initial-point so that light rays in zone 2 can become parallel to the optical axis when passing through this surface.

The spread angle for each group light rays is given by $\theta_a : \theta_b : \theta_c = 56^\circ : 10^\circ : 24^\circ$, which is determined by the intersection of surface ① and surface ④ and also surface ② and surface ③. The constructed 2D contour of the collimator lens is shown in Fig. 5. By rotating the contour about the optical axis, a 3D collimator lens is implemented as shown in Fig. 6.

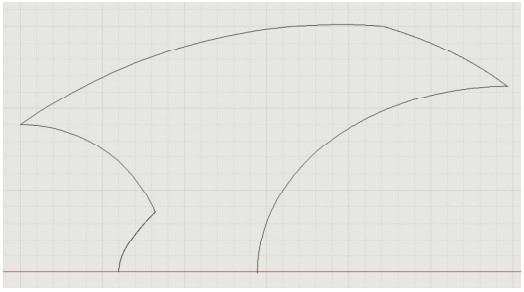

Fig. 5. Two-dimensional contour of the collimator lens.

#164581 - $15.00 USD Received 13 Mar 2012; revised 7 Apr 2012; accepted 7 Apr 2012; published 26 Apr 2012

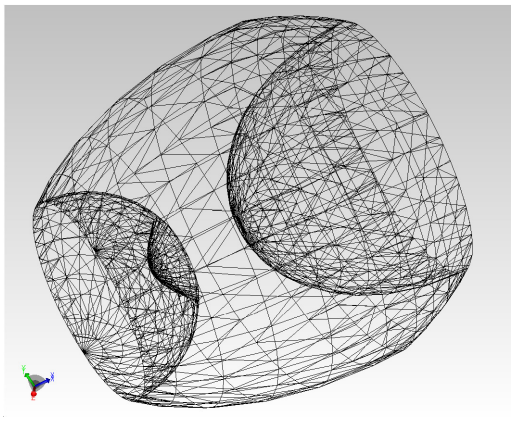

Fig. 6. Three-dimensional collimator lens.

3.2 Computer simulation

Though the compact collimator lens is constructed based on an ideal point source, to verify it also effective to a practical LED light source, a TracePro program is employed to trace one million light rays emitted from an LED through the lens. The associated simulation parameters of the collimator lens are given in Table 1, and the ray trace is shown in Fig. 7. To clearly see the deviation of the ray trace for a practical LED chip from that of a point source, both ray traces for the LED chip and point source are performed, and only five thousand rays are shown up, where Fig. 7(a) is the ray trace for the 1 mm × 1 mm LED chip and Fig. 7(b) is the ray trace for the point source. From Fig. 7(a), it can be seen that most of light rays emitted from the LED chip are collimated well by the lens; however, a small number of light rays deviate from the direction parallel to the optical axis. This phenomenon can be attributed to the non-ideal point source of the LED. However, Fig. 7(b) shows light rays from the point source can be collimated very well by this lens. Meanwhile, the main optical loss of the lens comes from the Fresnel loss and the absorption of the acrylic material, while some optical loss comes from the stray light as shown in Fig. 7(a). The associated illuminance map and distribution on a target plane at 6-m away are also shown in Fig. 8, which shows the spot size at 6-m away to be about 0.4 m. The rectangular candela distribution plot is shown in Fig. 9, which shows the beam angle is about 5 deg with total optical efficiency of 90.2% (referred to Fig. 8). In the computer simulation, the parameters, such as the material, the dimensions, and the shape of the lens, or the light distribution and chip size of the LED, affect the optical performance of the lens significantly, while the influence of the LED chip size is the most pronounced. Thus its effect on the optical efficiency and half view angles is investigated further. The simulation result is shown in Table 2, where the optical efficiency is represented in relative percentage. In addition, the optical efficiency versus the half view angle for different LED chip sizes is also plotted in Fig. 10. From the simulation results, it can be seen that the optical efficiency decreases with the LED chip size. For a 1.0 mm × 1.0 mm LED chip, the optical efficiency achieves 86.5% within a view angle of ± 5 deg. To obtain a reasonable optical efficiency, for example, 80% within a half view angle of 5 deg, the dimension of the LED chip should not be greater than 1.2 mm × 1.2 mm for a lens with aperture of 30 mm.

Table 1. Parameters of the Collimator Lens

Light source	1 mm × 1 mm LED chip
Total light-source flux	100 lm
Radiation pattern	Lambertian type
Lens aperture	30 mm
Lens material	Acrylic

#164581 - $15.00 USD Received 13 Mar 2012; revised 7 Apr 2012; accepted 7 Apr 2012; published 26 Apr 2012

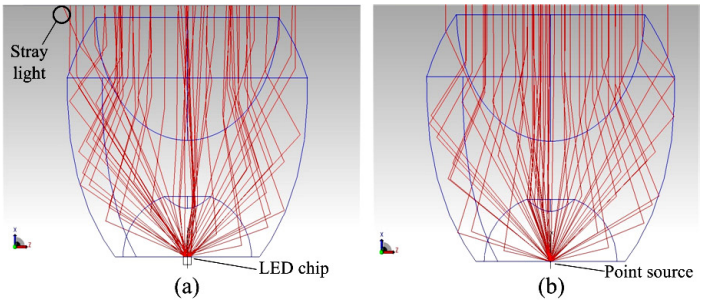

Fig. 7. Ray trace for (a) an LED light source and (b) a point source.

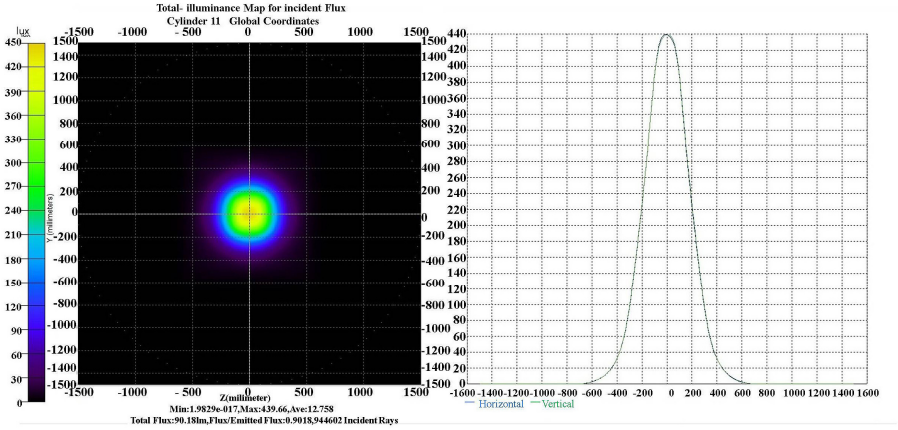

Fig. 8. The associated illuminance map and distribution on a target plane at 6-m away.

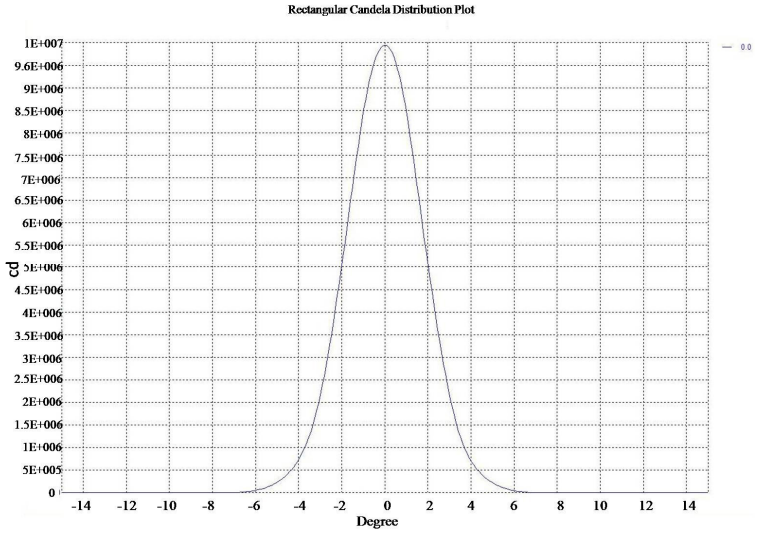

Fig. 9. The rectangular candela distribution plot.

#164581 - $15.00 USD Received 13 Mar 2012; revised 7 Apr 2012; accepted 7 Apr 2012; published 26 Apr 2012

Table 2. Percentage Optical Efficiency versus Different LED Chip Sizes and Half View Angles

Chip size (mm × mm)	Half view angle (deg)				
	1	2	3	4	5
0.2 × 0.2	86.91	90.60	90.61	90.62	90.62
0.4 × 0.4	60.33	86.89	90.43	90.60	90.61
0.6 × 0.6	35.32	76.04	86.77	89.94	90.51
0.8 × 0.8	22.46	60.15	80.08	86.65	89.37
1.0 × 1.0	14.97	45.70	70.87	81.73	86.50
1.2 × 1.2	10.27	35.34	59.93	75.43	82.54
1.4 × 1.4	7.57	27.89	48.89	67.81	77.80
1.6 × 1.6	5.81	22.46	41.79	59.60	72.06
1.8 × 1.8	4.60	18.26	35.32	52.01	65.55
2.0 × 2.0	3.77	14.95	30.17	45.49	59.13

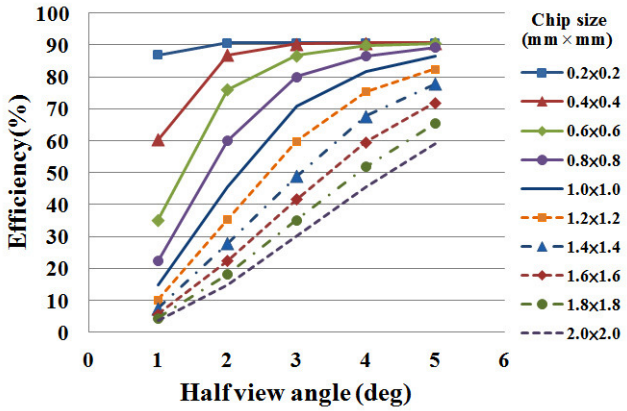

Fig. 10. The plot of optical efficiency versus the half view angle.

4. Practical measurement

In order to verify the optical performance of the collimator lens, a prototype in Fig. 11 is made; the candela distribution and the beam width versus distance are also measured. Both measurements proceed using an LED light source with measured flux of 47.89 lm and chip size less than1 mm × 1 mm, and the measurement results are shown in Figs. 12 and 13. Figure 12 gives the measured candela distribution, and Fig. 13 gives the beam width and the illuminance (on the optical axis) versus the distance. The measurement results demonstrate that a beam angle of 4.75 deg with overall optical efficiency of 90.3% (not shown in Figs. 12 and 13) and a beam width of 0.5 m at 6-m away are measured. Both data are very close to the simulation results in Section 3.2.

#164581 - $15.00 USD Received 13 Mar 2012; revised 7 Apr 2012; accepted 7 Apr 2012; published 26 Apr 2012

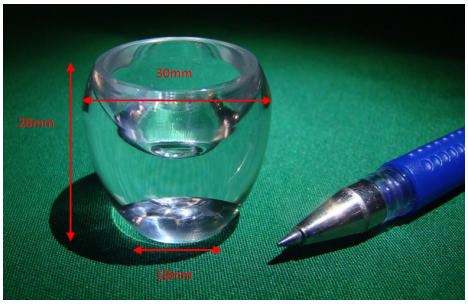

Fig. 11. The prototype of the collimator lens.

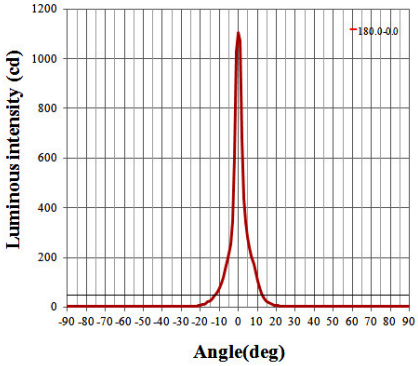

Fig. 12. The measured cardinal-angular intensity distribution.

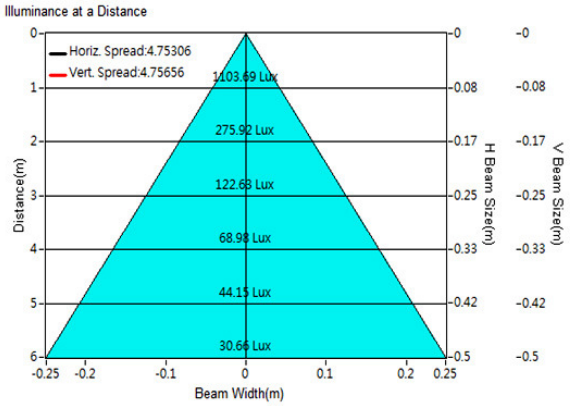

Fig. 13. The illuminance and beam width versus distance.

5. Conclusion

A freeform lens design method with the methodology based on basic geometric-optics analysis and construction approach is depicted in detail in this paper. As compared with existing methods in literatures, the derivative process of the method is simple and straightforward. This method can be used to design various indoor/outdoor LED luminaires for general or specific illumination applications. By employing this method, a novel and highly collimating LED lens with an aperture of 30 mm is constructed. The computer simulation results demonstrate that this lens can achieve a collimated beam with optical efficiency up to 86.5% under a view angle of ± 5 deg and a 1.0 mm × 1.0 mm LED chip. The chip-size dependent character of the collimator lens is also investigated. To obtain a

#164581 - $15.00 USD Received 13 Mar 2012; revised 7 Apr 2012; accepted 7 Apr 2012; published 26 Apr 2012

reasonable optical efficiency, the LED chip size should not be greater than 1.2 mm × 1.2 mm for a lens with aperture of 30 mm. In addition to the computer simulation, a practical measurement on a prototype of the lens is also conducted. The measurement results by using a LED with chip size less than 1 mm × 1 mm demonstrate that a beam angle of 4.75 deg with overall optical efficiency of 90.3% is obtained.

Acknowledgment

The authors would like to thank the National Science Council in Taiwan for financially supporting this research under Grant No. NSC 100-2221-E-018-004.

#164581 - $15.00 USD Received 13 Mar 2012; revised 7 Apr 2012; accepted 7 Apr 2012; published 26 Apr 2012